

## Supplementary Information for

### **Pliocene and Eocene provide best analogs for near-future climates**

Burke, K. D., Williams, J. W., Chandler, M. A., Haywood, A. M., Lunt, D. J., Otto-Bliesner, B. L.

Burke, K. D.

Email: [kdburke@wisc.edu](mailto:kdburke@wisc.edu)

#### **This PDF file includes:**

Supplementary Text

Figs. S1 to S14

Tables S1 to S3

Captions for Movies S1 to S8

References for Supplementary Information citations

#### **Other supplementary materials for this manuscript include the following:**

Movies S1 to S8

Supplementary Data and Code via Data Dryad

## Supplementary Text

### Corresponding projected climate analog results for RCP scenario 4.5

RCP4.5 commits the planet to a future global climate similar to that of the mid-Pliocene (Figs. S4, S5). The relative proportion of climate analogs shifts throughout the 21<sup>st</sup> century and remains nearly constant beyond 2100 CE when climate stabilization occurs. Changes in projected future climate analogs under RCP4.5 are predominantly driven by a change in future temperature, though precipitation is important for highly novel climates (e.g. monsoonal locations).

### Choice of Distance Metric

To assess the sensitivity of findings to selection of distance metric (1), Fig. S6 shows projected future climate analogs using an alternative distance metric, the standardized Euclidean distance (SED, *Materials and Methods*). Spatial patterns for both RCP4.5 and 8.5 are very similar to those reported using Mahalanobis Distance (Fig. 3). However, under RCP4.5, the Pliocene reaches a plurality by 2030 CE in the SED analyses rather than 2040 CE when Mahalanobis distance is used (Fig. S7). Under RCP8.5, the Pliocene reaches a plurality by 2020 CE in the SED analyses rather than 2030 CE. The Eocene reaches a plurality by 2150 CE with both distance metrics.

### Climate Zonal Means

Fig. S8 shows climate zonal means for the four indicator variables ( $T_{DJF}$ ,  $T_{JJA}$ ,  $P_{DJF}$ ,  $P_{JJA}$ ). These figures present a summary of the climate states used in our analyses, and contextualize their relative temperature and precipitation values. Mean values are calculated for 64 bins of latitude. If no terrestrial grid cells are present, the resulting value is NA. Zonal mean curves are then averaged across all models where there are multiple estimates of a given variable (i.e. at least two estimates of climate from the ensemble). Points are plotted using a loess smoothing method with a span of 0.125 (`ggplot2::geom_smooth`). Fig. S9 presents the individual variable means for GISS, HadCM, and CCSM.

### Novelty of Projected Future Climates

Fig. S10 shows the Mahalanobis climatic distance between the future climates at each location and its closest geohistorical climatic analog, drawn from any terrestrial location in the set of six potential climatic analogs. High minimum dissimilarities provide an index of the novelty of future climates relative to all considered geohistorical analogs. Fig. S11 shows the histogram of MD values for a comparison of historical to pre-industrial climates, used to identify the no-analog threshold (99<sup>th</sup> percentile). Values greater than 0.51102 for HadCM3, 0.36912 for GISS, and 0.39900 for CCSM indicate future climates with no close geohistorical analog (for SED, 6.09940 for HadCM3, 3.98705 for GISS, and 3.69044 for CCSM). Geologically novel climate tend to be centered in regions of high rainfall and temperature, e.g. in monsoonal systems and temperate coastal rainforests. By broadening the reference baseline to include multiple reference climate states from deep geological time, novelty values decrease, because there are more potential climates to find a best analog. Nevertheless, some future climates remain geologically novel.

### **Unique-Analog Analysis**

When matching future climates to potential geohistorical analogs, one question is whether the set of unique paleoclimatic analogs is small or large. “Unique” climatic analogs are unique in latitude, longitude, and time period. Future projections of climate contain the following number of terrestrial grid cells: 1909 (GISS), 1899 (HadCM), 1876 (CCSM), setting upper bounds to the possible number of unique paleoclimatic analogs for each future projection.

In both the RCP4.5 and RCP8.5 scenarios, the number of unique paleoclimatic analogs decreases over time, indicating that future climates are increasingly matching to a common subset of paleoclimatic analogs, which diminishes over time. By 2280 CE, under RCP4.5, the number of unique analogs reduces by 8.6% with GISS, 6.7% with HadCM, and 11.7% with CCSM (Fig. S12a). For RCP8.5, the reductions are larger, reaching 28.9% with GISS, 40.1% with HadCM, and 40.6% with CCSM by 2280 CE (Fig. S12b). The sharper reduction under RCP8.5 because of the larger future climate changes increasingly moves some climates beyond the bounds of the geohistorical pool of climate analogs, causing multiple future climate locations to match to a smaller subset of climate analogs at the edge of paleoclimatic space.

### **Distance to Closest Climate Analog**

Analogues for projected future climates tend not to be found locally (i.e. from the same grid location). For the occasional climate that does match to the same grid location, or a close-by grid location, it is important to consider the temporal dimension of this analog. Consider projected Arctic climates for 2100 CE under RCP8.5 (across all models)- the majority of analogs are found outside of this region. Even temporally close analogs (Historical and pre-industrial) tend to be sourced from across the subarctic or alpine regions of the world (Fig. S13). As climate continues to change, geographic distances to closest analogs tend to increase (Fig. S14). This is likely due to the continuing climatic change, and the increasing prevalence of temporally distant analogs from different paleogeographies.

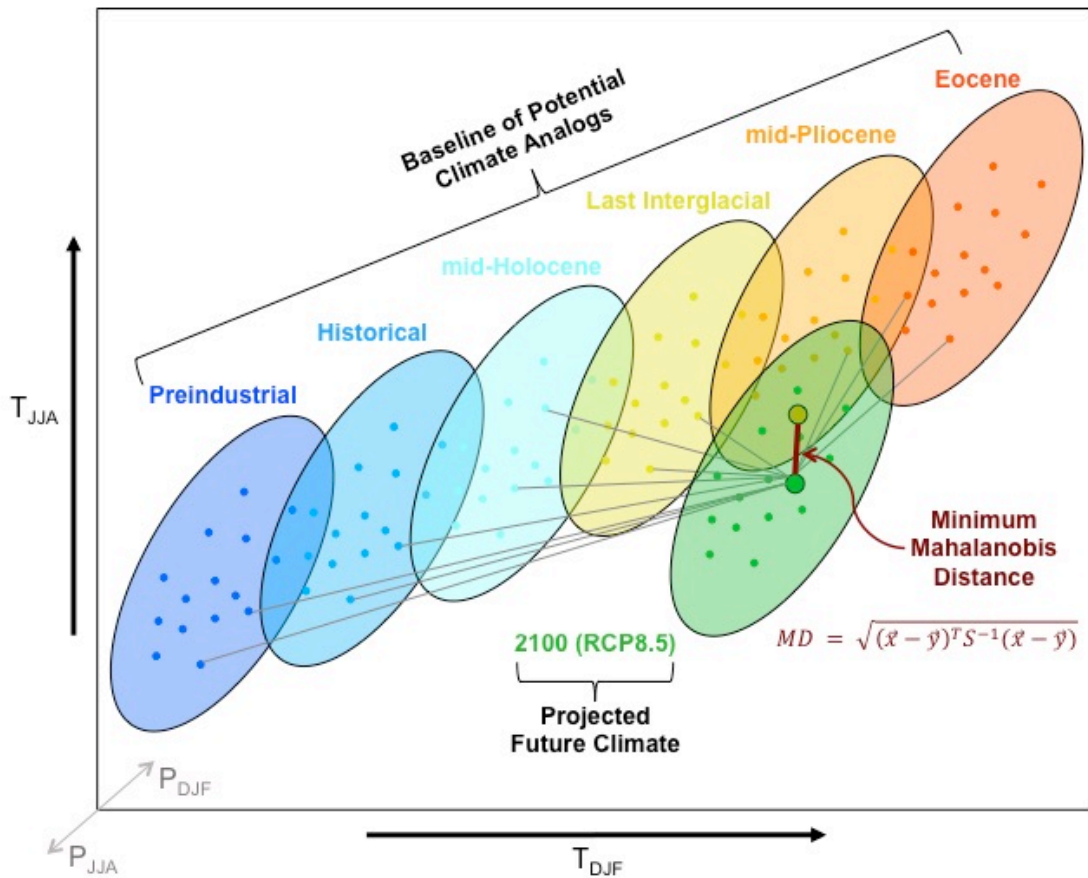


**Fig. S1. Schematic representation of climate analog methodology.** Each terrestrial grid location from a projected future climatology is compared to a reference baseline of past climates that comprises the climates at all terrestrial grid locations, across all geohistorical baselines. Here, a 30-year climatology centered on the year 2100 CE is compared to the reference baseline. The minimum MD represents the closest analog climate, shown here in red, which is identified as a mid-Pliocene analog. Relative positioning of time periods is for illustrative purposes only.

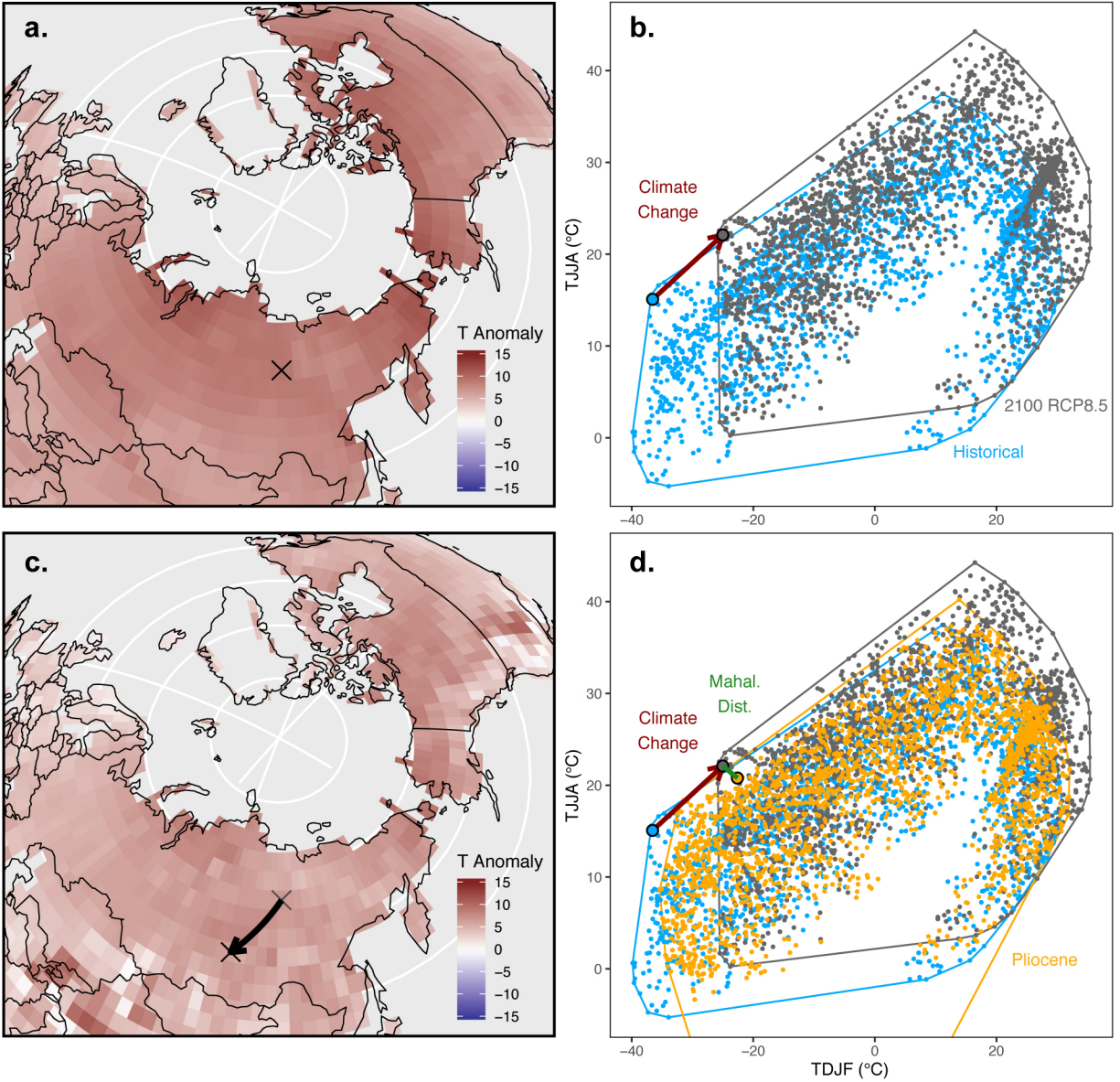


**Fig. S2. Matching future climates to their closest geohistorical analogs.** Shown here for a grid location in Eurasia and its climate at 2100 CE (RCP8.5; CCSM), which matches most closely to a climate from the Pliocene. Local temperature change at each grid location (a) is shown as red background and is based on the mean difference of  $T_{DJF}$  and  $T_{JJA}$  between 2100 CE and the historical era (1940-1970 CE). The trajectory in climate space for that grid location between the historical era (blue points) and 2100 CE (gray points) indicates warming (b). The spatial location of the closest Pliocene analog is identified (c), with a backdrop of Pliocene temperature anomalies relative to the historical era. The distance to the closest analog selected from Pliocene (orange) is shown in climate space (d). All analyses in the text and SI Appendix include seasonal temperature and precipitation, however only temperature is shown here for simplicity.

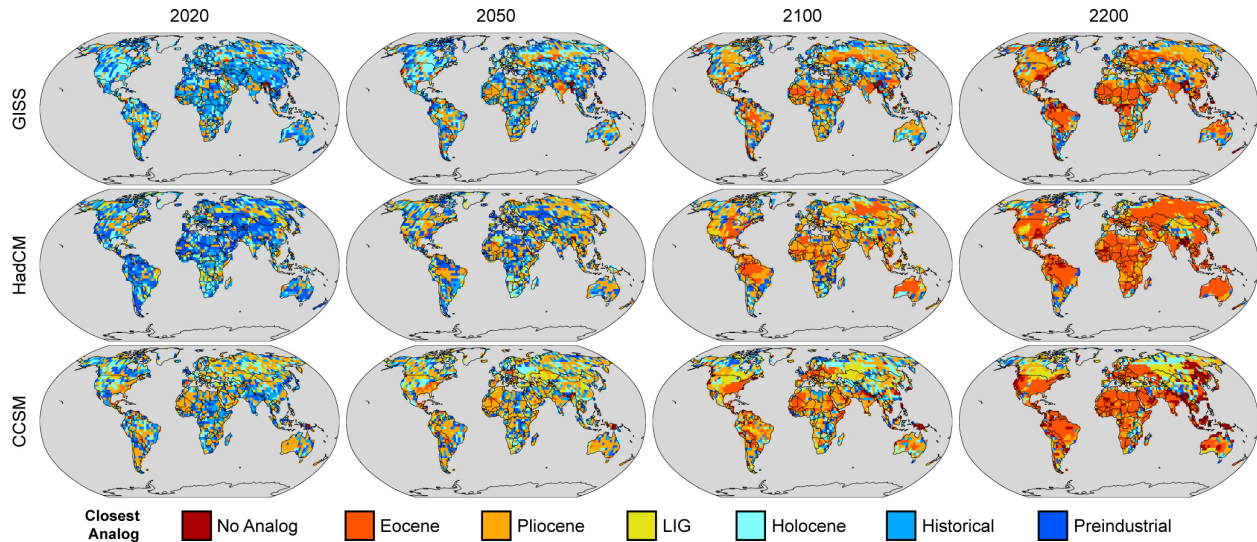


**Fig. S3. Projected geographic distribution of future climate analogs (RCP8.5).** Future climate analogs for 2020, 2050, 2100, and 2200 CE according to the GISS, HadCM, and CCSM earth system models. Each location is color coded according to the reference geohistorical baseline state from which its closest climatic analog was sourced. Figure design follows Fig. 3 in main text. See also animations available as Movies S1-S3.

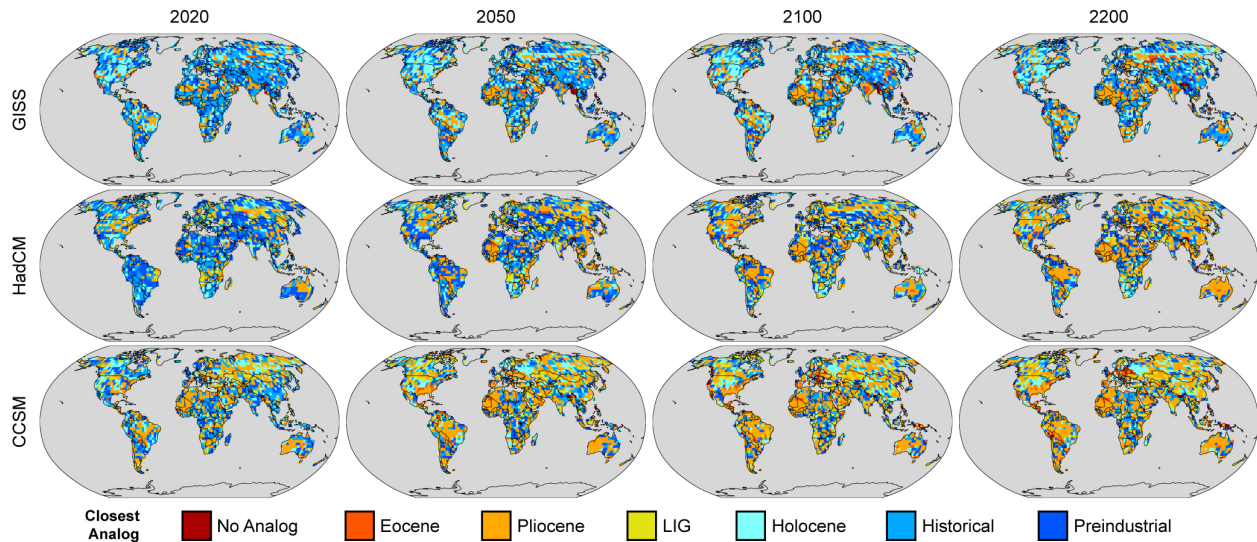


**Fig. S4. Projected geographic distribution of future climate analogs (RCP4.5).** Future climate analogs for 2020, 2050, 2100, and 2200 CE according to the GISS, HadCM, and CCSM earth system models. Each location is color coded according to the reference geohistorical baseline state from which its closest climatic analog was sourced. Figure design follows Fig. 3 in main text. See also animations available as Movies S4-S6.

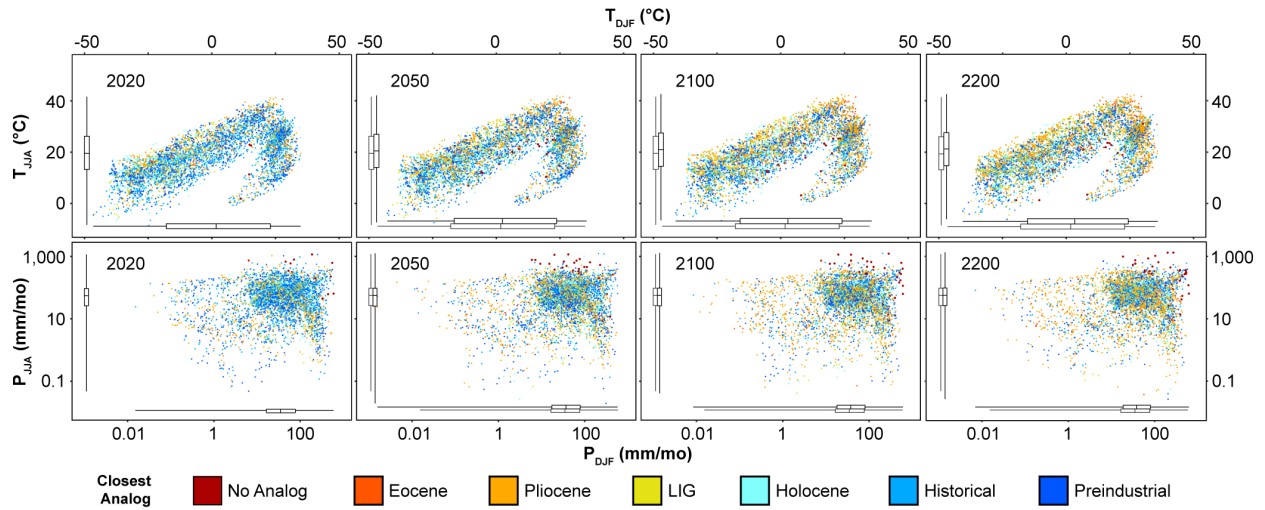


**Fig. S5. Projected future climate space by closest analog (RCP 4.5).** Top row: DJF vs. JJA temperature space. Bottom: DJF vs. JJA precipitation space. Each point represents a terrestrial grid location from the model ensemble, for the specified decade in the RCP4.5 projection. Points are color-coded according to the geohistorical climate that their closest analog sources from. Box-and-whisker plots show the data range, median, and 1<sup>st</sup> and 3<sup>rd</sup> quartiles for two time periods: the specified decade (black) and 2020 CE for reference (grey). Figure design follows Fig. 4 in main text.

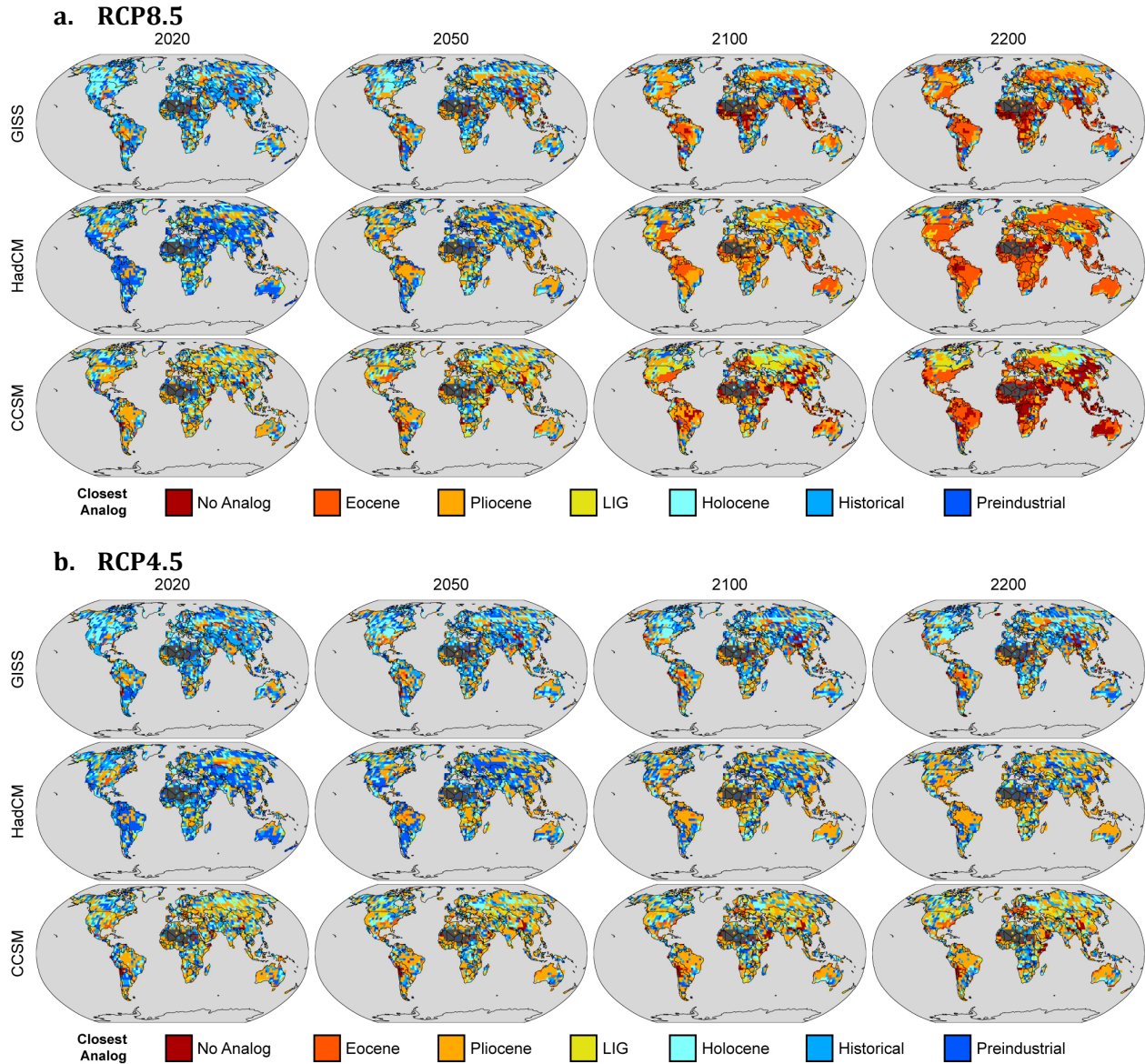


**Fig. S6. Projected geographic distribution of future climate analogs using standardized Euclidean distance.** Future climate analogs for 2020, 2050, 2100, and 2200 CE according to the GISS, HadCM, and CCSM earth system models for RCP4.5 (a) and RCP8.5 (b). Each location is color coded according to the reference geohistorical baseline state from which its closest climatic analog was sourced. Figure design follows Fig. 3 in main text.

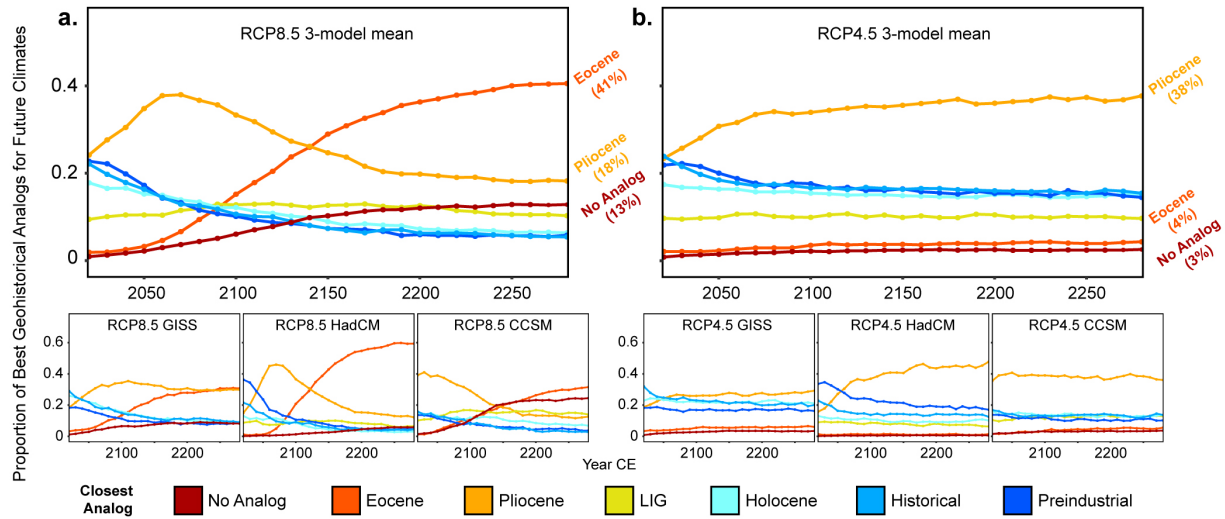


**Fig. S7. Time series of the closest geohistorical climatic analogs for projected climates, 2020 to 2280 CE (SED).** Colored lines indicate the proportion of terrestrial grid cells for each future decade with the closest climatic match to climates from six potential geohistorical climate analogs: early Eocene, mid-Pliocene, Last Interglacial (LIG), mid-Holocene, historical (1940-1970 CE), and pre-industrial (1850 CE) for RCP8.5 (a) and RCP4.5 (b). No LIG simulation from GISS was available at time of analysis. Red line indicates proportion of future climates that are geologically novel. Results reflect analyses using SED rather than MD.

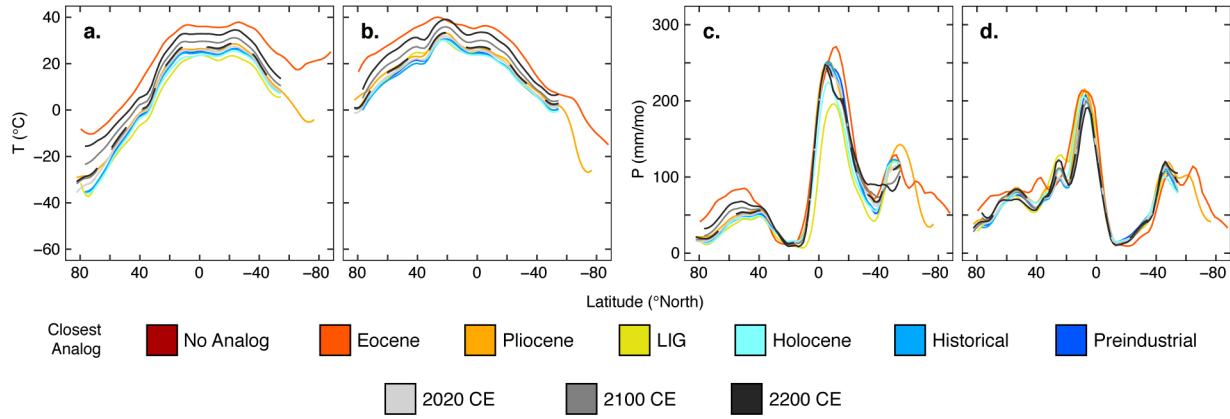
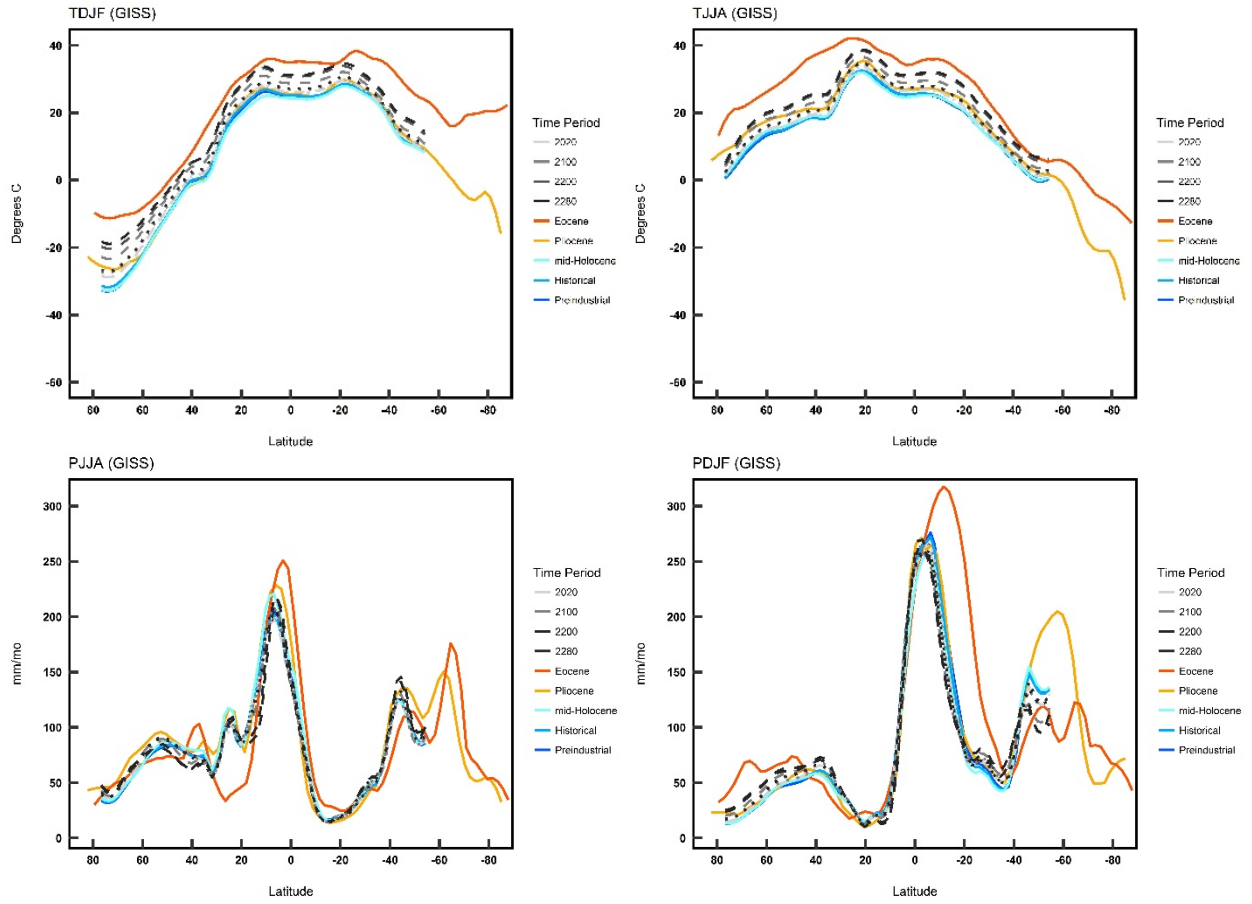
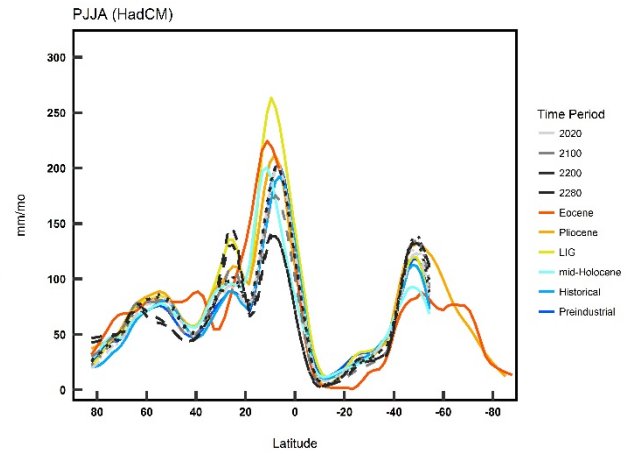
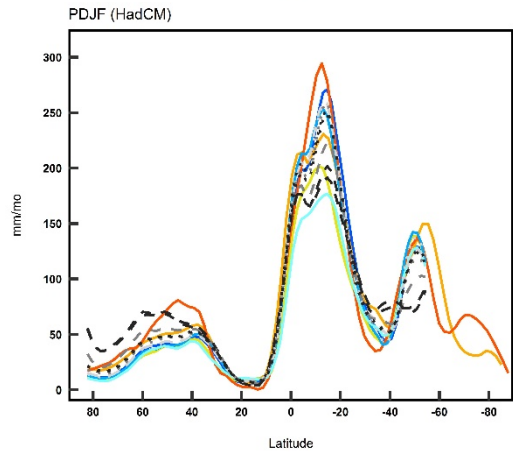
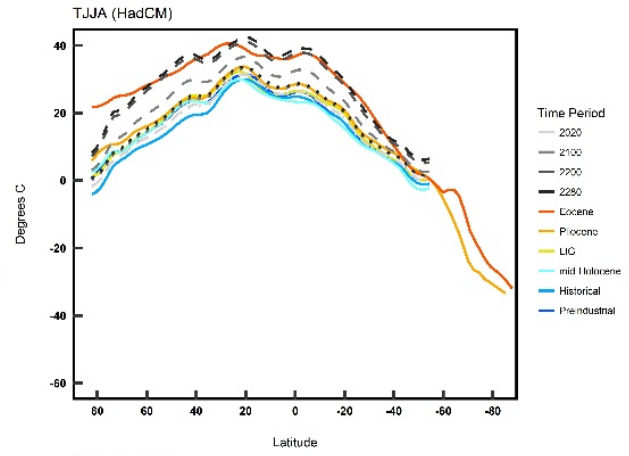
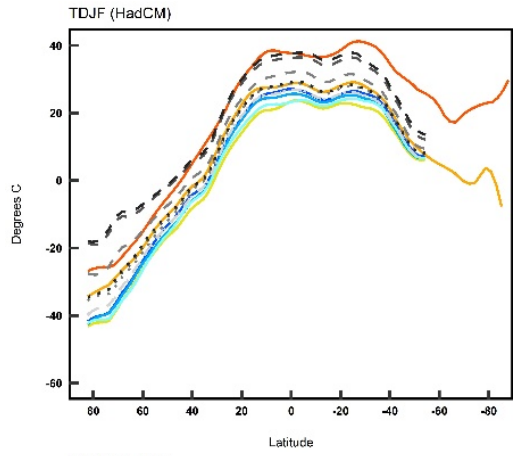


**Fig. S8. Zonal means for RCP scenarios and reference paleoclimates.** Zonal means of near-surface air temperature ( $^{\circ}\text{C}$ ) for DJF (a) and JJA (b). Zonal means of monthly precipitation (mm/month) for DJF (c) and JJA (d). Colored lines correspond to the individual means of the six reference climates included in analyses. The grey-to-black lines correspond to three time periods from the RCP future scenarios (RCP4.5: dashed lines, RCP8.5: solid lines). All four panels show the three-model ensembles from each earth system model.

**a. GISS**



## b. HadCM



**c. CCSM**

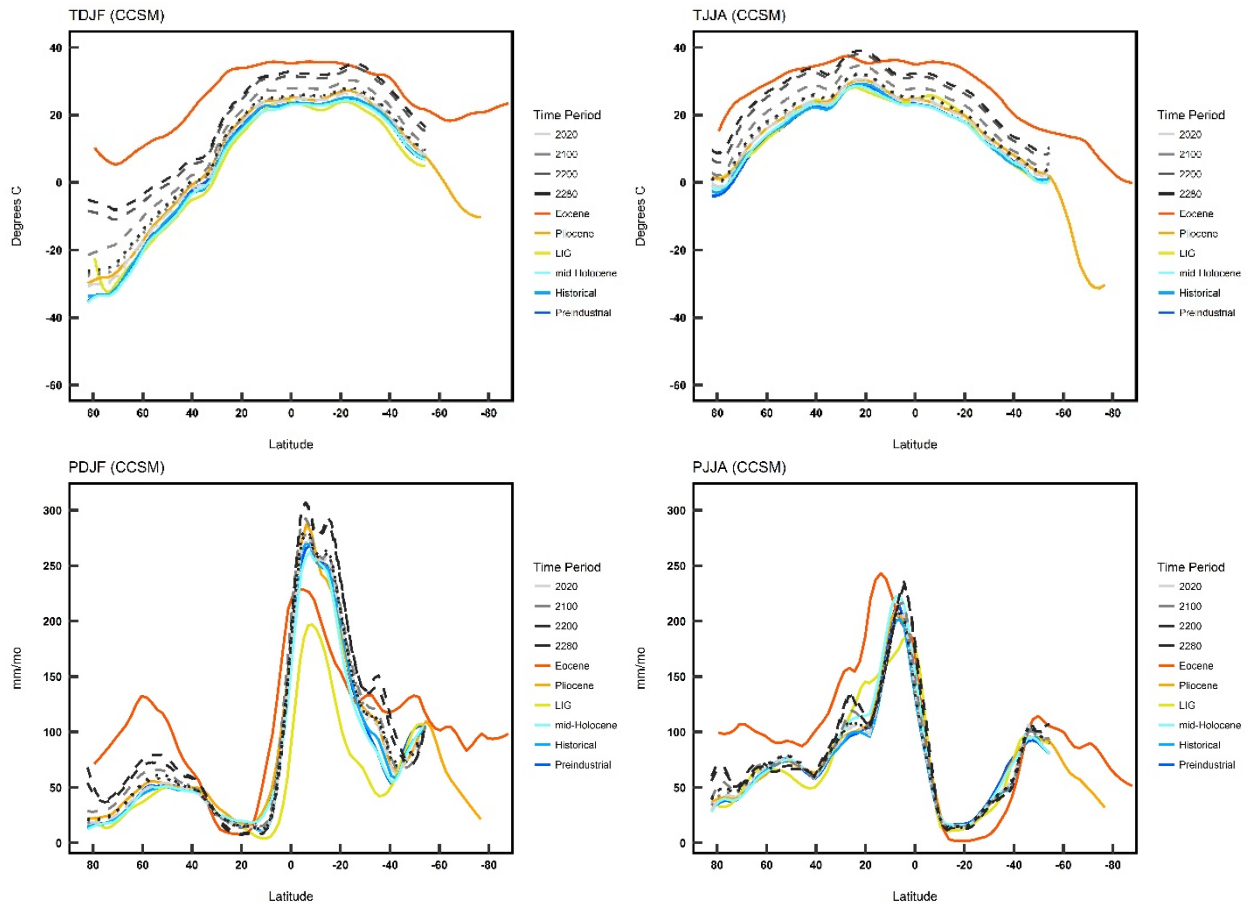


**Fig. S9. Climate zonal means for individual earth system model families.** Zonal means of near-surface air temperature ( $^{\circ}\text{C}$ ) for DJF and JJA and of monthly precipitation (mm/month) for DJF and JJA for GISS (a), HadCM (b) and CCSM (c). Colored lines correspond to the individual means of the six reference climates included in analyses. The grey-to-black lines correspond to four time periods (2020, 2100, 2200, 2280 CE, respectively) from RCP-driven future simulations (RCP4.5 as dots, RCP8.5 as long-dashes).

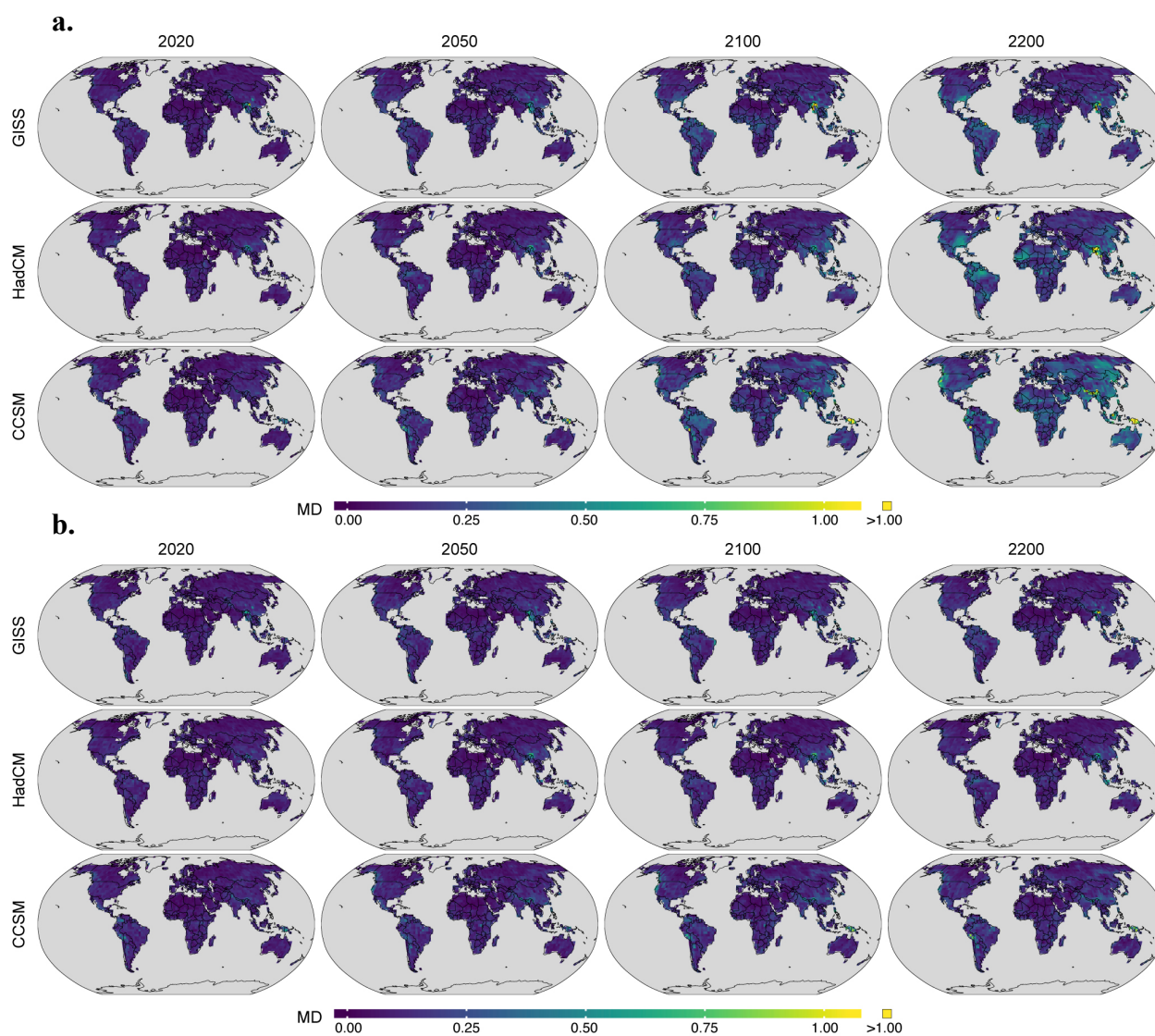


**Fig. S10. Projected future climate novelty.** Maps of the Mahalanobis distance of future projected climates to their closest analog from six geohistorical reference baselines for RCP8.5 (a) and RCP4.5 (b). The color gradient from zero to one corresponds to the ~99th percentile of MD values across individual models under the RCP8.5 scenario.

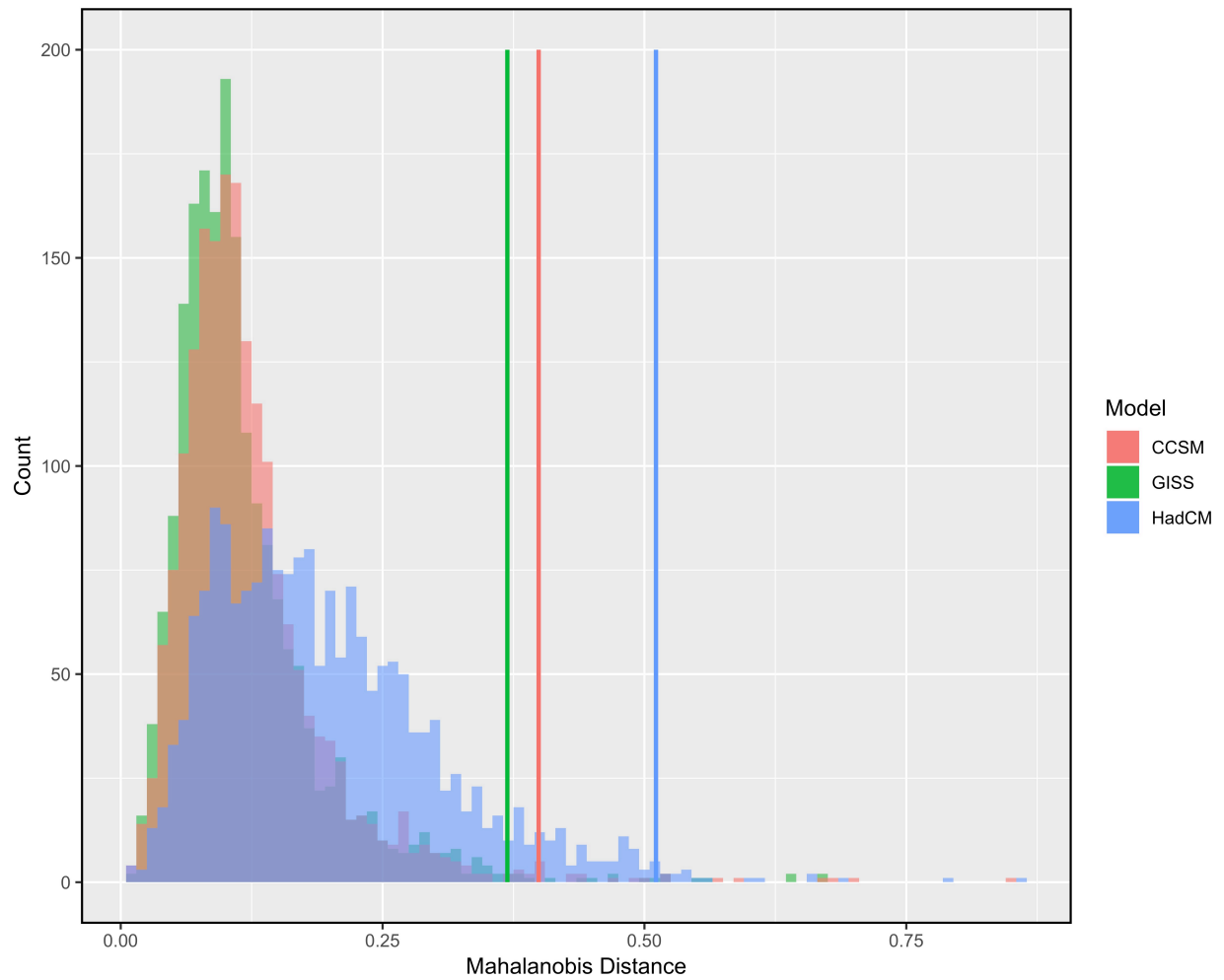


**Fig. S11. Histograms of Mahalanobis distance for no analog threshold.** The 99<sup>th</sup> percentile of MD values from a comparison of Historical to pre-industrial climates was used to determine the no analog threshold for each model family. Histograms and thresholds (vertical lines) are presented for each model family.

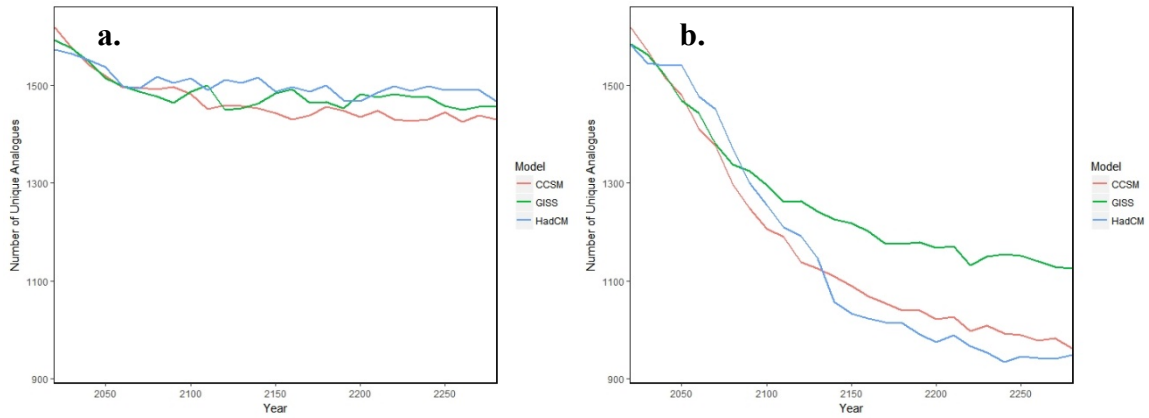


**Fig. S12. Decline in number of unique climate analogs.** The number of unique climate analogs declines by 2280 CE for RCP4.5 (a), and particularly for RCP8.5 (b).

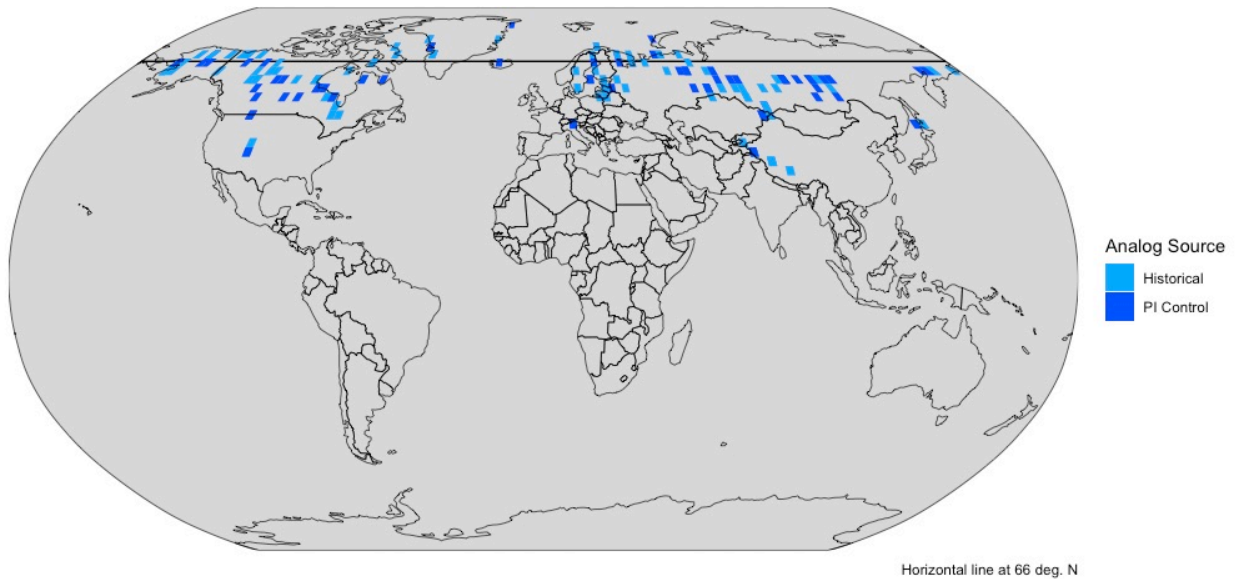


**Fig. S13. Spatial location of Arctic climate analogs for 2100 CE (RCP8.5; full ensemble).** Historical and pre-industrial climate analogs for the Arctic region (grid locations north of 66° N) tend to originate across the subarctic, and extend into alpine regions throughout the mid-latitudes.

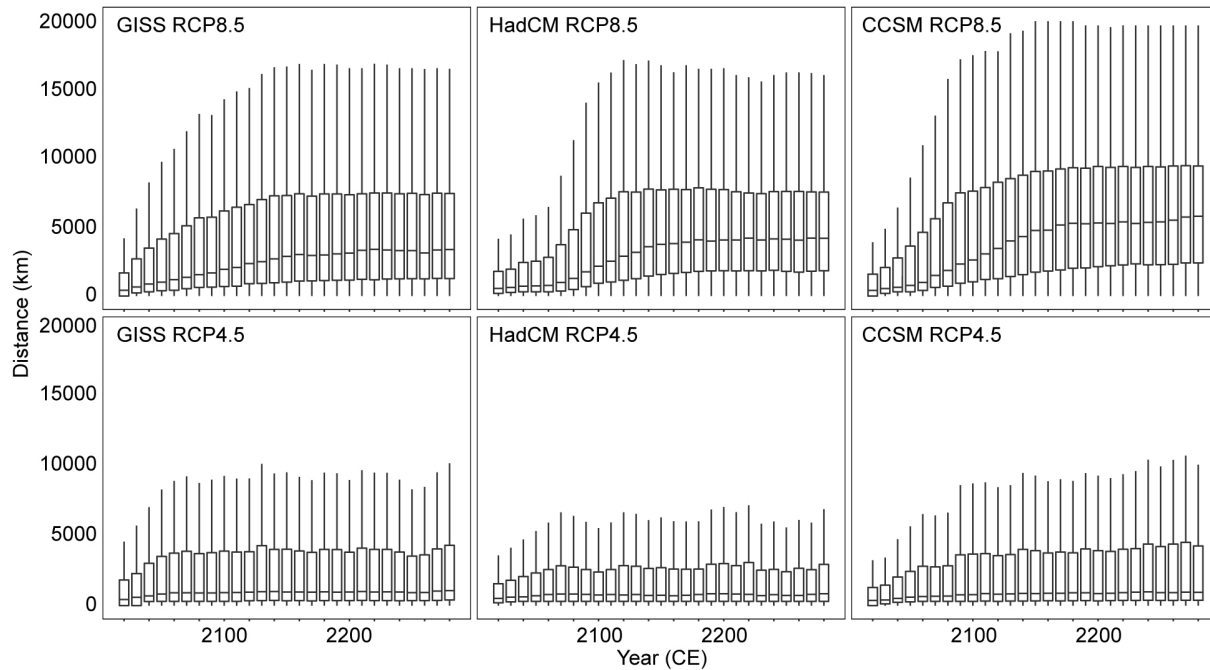


**Fig. S14. Geographic distances to closest climate analogs.** The distribution of geographic distances for projected climates and their geohistorical analogs increases over time. Boxplots, shown here for each decade from 2020-2280 CE, indicate the median (horizontal line), 1<sup>st</sup> and 3<sup>rd</sup> quartile (box), and range (Q1 – 1.5\*interquartile range, Q3 + 1.5\*interquartile range) of geographic distances for all grid locations in each time slice. Outliers exceeding this range are not shown.

**Table S1. Earth system model simulations and relevant details**

Time Period	Model Group	Model Configuration	Individual Reference*	Additional References	Atmosphere Resolution (lon×lat×vert)
RCP8.5	CCSM	CCSM4	b40.rcp8_5.1deg.001 (2)	(3, 4)	288 × 192 × 26
	GISS	ModelE2-R	r1i1p1 (5)	(6)	144 × 90 × 40
	HadCM	HadCM3-M1-E	Tdlac (7)	(8–10)	96 × 73 × 19
RCP4.5	CCSM	CCSM4	b40.rcp4_5.1deg.001 (2)	(3, 4)	288 × 192 × 26
	GISS	ModelE2-R	r1i1p1 (5)	(6)	144 × 90 × 40
	HadCM	HadCM3-M1-E	Tdlah (7)	(8–10)	96 × 73 × 19
Historical	CCSM	CCSM4	b40.20th.track1.1deg.008	(3, 4)	288 × 192 × 26
	GISS	ModelE2-R	r1i1p1 (11)	(6)	144 × 90 × 40
	HadCM	HadCM3-M1-E	r1i1p1 (7)	(8–10)	96 × 73 × 19
Pre-industrial	CCSM	CCSM4	b40.1850.track1.1deg.006	(3, 4)	288 × 192 × 26
	GISS	ModelE2-R	r1i1p142 (11)	(6)	144 × 90 × 40
	HadCM	HadCM3-M2-D	PMIP2_0K_OAV (12)	(8–10)	96 × 73 × 19
mid-Holocene	CCSM	CCSM4	b40.mh6ka.1deg.003	(3, 4)	288 × 192 × 26
	GISS	ModelE2-R	r1i1p1	(6)	144 × 90 × 40
	HadCM	HadCM3-M2-D	PMIP2_6K_OAV (12)	(8–10)	96 × 73 × 19
LIG	CCSM	CCSM3	b30.137 (13)	(14)	256 × 128 × 26
	GISS	NA	NA	NA	NA
	HadCM	HadCM3-M1-E	Tdwz (15)	(8–10)	96 × 73 × 19
mid-Pliocene	CCSM	CCSM4	b40.plio.FV1.003 (16)	(3, 4)	288 × 192 × 26
	GISS	ModelE2-R	r1i1p5 (17)	(6)	144 × 90 × 40
	HadCM	HadCM3-M1-E	Tczy (18)	(8–10)	96 × 73 × 19
early Eocene	CCSM	CCSM3	k.EO4.02.t42 (19)	(14)	128 × 64 × 26
	GISS	ModelE-R	(20)	(21)	72 × 46 × 20
	HadCM	HadCM3-M2.2-E	Tbpiga (22)	(8–10)	96 × 73 × 19

\*Relevant publication information provided when available in addition to internal experiment/case name. For ‘rip’ codes the nomenclature is as follows: r for realization, i for initialization, p for physics, followed by an integer.

**Table S2. Earth system model access**

Time Period	Model Group	Agency	Source
RCP8.5	CCSM	World Climate Research Programme	<a href="https://esgf-node.llnl.gov/projects/esgf-llnl/">https://esgf-node.llnl.gov/projects/esgf-llnl/</a>
	GISS	World Climate Research Programme	<a href="https://esgf-node.llnl.gov/projects/esgf-llnl/">https://esgf-node.llnl.gov/projects/esgf-llnl/</a>
	HadCM	Bristol Research Initiative for the Dynamic Global Environment*	<a href="http://www.bridge.bris.ac.uk/resources/simulations">http://www.bridge.bris.ac.uk/resources/simulations</a>
RCP4.5	CCSM	World Climate Research Programme	<a href="https://esgf-node.llnl.gov/projects/esgf-llnl/">https://esgf-node.llnl.gov/projects/esgf-llnl/</a>
	GISS	World Climate Research Programme	<a href="https://esgf-node.llnl.gov/projects/esgf-llnl/">https://esgf-node.llnl.gov/projects/esgf-llnl/</a>
	HadCM	Bristol Research Initiative for the Dynamic Global Environment	<a href="http://www.bridge.bris.ac.uk/resources/simulations">http://www.bridge.bris.ac.uk/resources/simulations</a>
Historical	CCSM	World Climate Research Programme	<a href="https://esgf-node.llnl.gov/projects/esgf-llnl/">https://esgf-node.llnl.gov/projects/esgf-llnl/</a>
	GISS	World Climate Research Programme	<a href="https://esgf-node.llnl.gov/projects/esgf-llnl/">https://esgf-node.llnl.gov/projects/esgf-llnl/</a>
	HadCM	World Climate Research Programme	<a href="https://esgf-node.llnl.gov/projects/esgf-llnl/">https://esgf-node.llnl.gov/projects/esgf-llnl/</a>
Pre-industrial	CCSM	World Climate Research Programme	<a href="https://esgf-node.llnl.gov/projects/esgf-llnl/">https://esgf-node.llnl.gov/projects/esgf-llnl/</a>
	GISS	World Climate Research Programme	<a href="https://esgf-node.llnl.gov/projects/esgf-llnl/">https://esgf-node.llnl.gov/projects/esgf-llnl/</a>
	HadCM	PMIP2 <sup>†</sup>	
mid-Holocene	CCSM	World Climate Research Programme	<a href="https://esgf-node.llnl.gov/projects/esgf-llnl/">https://esgf-node.llnl.gov/projects/esgf-llnl/</a>
	GISS	World Climate Research Programme	<a href="https://esgf-node.llnl.gov/projects/esgf-llnl/">https://esgf-node.llnl.gov/projects/esgf-llnl/</a>
	HadCM	World Climate Research Programme	<a href="https://esgf-node.llnl.gov/projects/esgf-llnl/">https://esgf-node.llnl.gov/projects/esgf-llnl/</a>
LIG	CCSM	Earth System Grid	<a href="https://www.earthsystemgrid.org/">https://www.earthsystemgrid.org/</a>
	GISS	NA	NA
	HadCM	Bristol Research Initiative for the Dynamic Global Environment	<a href="http://www.bridge.bris.ac.uk/resources/simulations">http://www.bridge.bris.ac.uk/resources/simulations</a>
mid-Pliocene	CCSM	World Climate Research Programme	<a href="https://esgf-node.llnl.gov/projects/esgf-llnl/">https://esgf-node.llnl.gov/projects/esgf-llnl/</a>
	GISS	Authors of 17	Reference 17
	HadCM	Bristol Research Initiative for the Dynamic Global Environment	<a href="http://www.bridge.bris.ac.uk/resources/simulations">http://www.bridge.bris.ac.uk/resources/simulations</a>
early Eocene	CCSM	Supplementary Information	Reference 19
	GISS	Authors of 23	Reference 23
	HadCM	Bristol Research Initiative for the Dynamic Global Environment	<a href="http://www.bridge.bris.ac.uk/resources/simulations">http://www.bridge.bris.ac.uk/resources/simulations</a>

\*Simulations from the BRIDGE HadCM family of models are available from the World Climate Research Programme. However, to maintain consistency in model comparisons, we restricted our use to only the HadCM3 version of simulations, which was unavailable there.

<sup>†</sup>We use the pre-industrial simulation associated with PMIP2, which corresponds to boundary conditions *ca.* 1850 CE. The PMIP3 simulation available from the World Climate Research Programme uses boundary conditions *ca.* 850 CE.

**Table S3. Percentage of grid cells identified as geologically novel**

	<b>2020</b>	<b>2050</b>	<b>2100</b>	<b>2150</b>	<b>2200</b>	<b>2250</b>	<b>2280</b>
<b>RCP4.5</b>							
GISS	0.4	0.8	0.9	0.8	0.9	0.6	0.9
HadCM3	0.0	0.2	0.1	0.2	0.3	0.2	0.1
CCSM	0.3	0.6	1.0	0.9	1.0	1.4	1.4
<b>RCP8.5</b>							
GISS	0.5	1.0	2.1	3.8	4.1	5.3	5.2
HadCM3	0.1	0.2	0.4	1.2	2.7	4.6	5.4
CCSM	0.4	0.9	3.8	8.8	13.0	16.5	15.3

**Movie S1. CCSM Climate Analog Animation (RCP8.5).** This animation shows the spatial distribution of future climate analogs under RCP8.5 for CCSM. Each decade from 2020 to 2280 CE is shown, and locations are color-coded according to the reference geohistorical state from which their closest climatic analog was sourced.

**Movie S2. HadCM Climate Analog Animation (RCP8.5).** This animation shows the spatial distribution of future climate analogs under RCP8.5 for HadCM. Each decade from 2020 to 2280 CE is shown, and locations are color-coded according to the reference geohistorical state from which their closest climatic analog was sourced.

**Movie S3. GISS Climate Analog Animation (RCP8.5).** This animation shows the spatial distribution of future climate analogs under RCP8.5 for GISS. Each decade from 2020 to 2280 CE is shown, and locations are color-coded according to the reference geohistorical state from which their closest climatic analog was sourced. No simulation of the Last Interglacial was available for GISS at time of publication.

**Movie S4. CCSM Climate Analog Animation (RCP4.5).** This animation shows the spatial distribution of future climate analogs under RCP4.5 for CCSM. Each decade from 2020 to 2280 CE is shown, and locations are color-coded according to the reference geohistorical state from which their closest climatic analog was sourced.

**Movie S5. HadCM Climate Analog Animation (RCP4.5).** This animation shows the spatial distribution of future climate analogs under RCP4.5 for HadCM. Each decade from 2020 to 2280 CE is shown, and locations are color-coded according to the reference geohistorical state from which their closest climatic analog was sourced.

**Movie S6. GISS Climate Analog Animation (RCP4.5).** This animation shows the spatial distribution of future climate analogs under RCP4.5 for GISS. Each decade from 2020 to 2280 CE is shown, and locations are color-coded according to the reference geohistorical state from which their closest climatic analog was sourced. No simulation of the Last Interglacial was available for GISS at time of publication.

**Movie S7. Median Climate Analog Animation (RCP8.5).** This animation shows the spatial distribution of future climate analogs under RCP8.5 for the ensemble median. Each decade from 2020 to 2280 CE is shown, and locations are color-coded according to the reference geohistorical state from which their closest climatic analog was sourced.

**Movie S8. Median Climate Analog Animation (RCP4.5).** This animation shows the spatial distribution of future climate analogs under RCP4.5 for the ensemble median. Each decade from 2020 to 2280 CE is shown, and locations are color-coded according to the reference geohistorical state from which their closest climatic analog was sourced.

## References

1. Mahony CR, Cannon AJ, Wang T, Aitken SN (2017) A closer look at novel climates: new methods and insights at continental to landscape scales. *Glob Chang Biol* 23:3934–3955.
2. Meehl GA, et al. (2012) Climate system response to external forcings and climate change projections in CCSM4. *J Clim* 25:3661–3683.
3. Gent PR, et al. (2011) The community climate system model version 4. *J Clim* 24:4973–4991.
4. Danabasoglu G, et al. (2012) The CCSM4 ocean component. *J Clim* 25:1361–1389.
5. Nazarenko L, et al. (2015) Future climate change under RCP emission scenarios with GISS ModelE2. *J Adv Model Earth Syst* 7:244–267.
6. Schmidt GA, et al. (2014) Configuration and assessment of the GISS ModelE2 contributions to the CMIP5 archive. *J Adv Model Earth Syst* 6:141–184.
7. Collins M, Tett SFB, Cooper C (2001) The internal climate variability of HadCM3, a version of the Hadley Centre coupled model without flux adjustments. *Clim Dyn* 17:61–81.
8. Valdes PJ, et al. (2017) The BRIDGE HadCM3 family of climate models: HadCM3@Bristol v1.0. *Geosci Model Dev* 10:3715--3743.
9. Pope VD, Gallani ML, Rowntree PR, Stratton R a. (2000) The impact of new physical parametrizations in the Hadley Centre climate model: HadAM3. *Clim Dyn* 16:123–146.
10. Gordon C, et al. (2000) The simulation of SST, sea ice extents and ocean heat transports in a version of the Hadley Center coupled model without flux adjustments. *Clim Dyn* 16:147–168.
11. Miller RL, et al. (2014) CMIP5 historical simulations (1850–2012) with GISSModelE2. *J Adv Model Earth Syst* 6:441–478.
12. Braconnot P, et al. (2007) Results of PMIP2 coupled simulations of the Mid-Holocene and Last Glacial Maximum - Part 1: experiments and large-scale features. *Clim Past* 3:261–277.
13. Otto-Bliesner BL, et al. (2013) How warm was the last interglacial? New model-data comparisons. *Philos Trans R Soc A* 371.
14. Collins WD, et al. (2006) The Community Climate System Model version 3 (CCSM3). *J Clim* 19:2122–2143.
15. Singarayer JS, Valdes PJ (2010) High-latitude climate sensitivity to ice-sheet forcing over the last 120 kyr. *Quat Sci Rev* 29:43–55.
16. Rosenbloom N a., Otto-Bliesner BL, Brady EC, Lawrence PJ (2013) Simulating the mid-Pliocene Warm Period with the CCSM4 model. *Geosci Model Dev* 6:549–561.
17. Chandler MA, Sohl LE, Jonas JA, Dowsett HJ, Kelley M (2013) Simulations of the mid-Pliocene Warm Period using two versions of the NASA/GISS ModelE2-R Coupled Model. *Geosci Model Dev* 6:517–531.
18. Lunt DJ, et al. (2010) Earth system sensitivity inferred from Pliocene modelling and data. *Nat Geosci* 3:60–64.
19. Huber M, Caballero R (2011) The early Eocene equable climate problem revisited. *Clim Past* 7:603–633.
20. Roberts CD, LeGrande AN, Tripathi AK (2009) Climate sensitivity to Arctic seaway

- restriction during the early Paleogene. *Earth Planet Sci Lett* 286:576–585.
21. Schmidt GA, et al. (2006) Present-day atmospheric simulations using GISS ModelE: Comparison to in-situ, satellite and reanalysis data. *J Clim* 19:153–192.
  22. Lunt DJ, et al. (2010) CO<sub>2</sub>-driven ocean circulation changes as an amplifier of Paleocene-Eocene thermal maximum hydrate destabilization. *Geology* 38:875–878.
  23. Carmichael MJ, et al. (2016) A model-model and data-model comparison for the early Eocene hydrological cycle. *Clim Past* 12:455–481.